

## ARTICLE

# Unravelling the Binding Affinity and Selectivity of Molybdenum (II) Phenanthroline Complexes with DNA G-Quadruplexes by Using Linear-Scaling DFT Studies. The Important Role of the Ancillary Ligands

Received 00th January 20xx,  
Accepted 00th January 20xx

DOI: 10.1039/x0xx00000x

Iker Ortiz de Luzuriaga,<sup>a,b</sup> Ángel Sanchez-Gonzalez,<sup>c</sup> Wojciech Synoradzki,<sup>c</sup> Xabier Lopez,<sup>b,d</sup> and Adrià Gil<sup>\*a,c,e,f</sup>

We have used near linear-scaling density functional theory (LS-DFT) methods including dispersion, for the first time, to study the interaction of two isomers, equatorial (Eq) and axial (Ax), of the  $[\text{Mo}(\eta^3\text{-C}_3\text{H}_5)\text{Br}(\text{CO})_2(\text{phen})]$  metal complex with the DNA G-quadruplexes (GQ) to gain insight on its cytotoxicity. The LMKLL/DZDP level of calculation, which includes van der Waals contributions, with the SIESTA software was used to treat by means of first-principles computations the whole biological studied model system with  $\sim 1000$  atoms. Computed formation energies point to systems containing the Ax isomer as the most stable although the nearest system in energy containing the Eq isomer is only 7.5 kcal mol<sup>-1</sup> above. On the other hand, the energy decomposition analysis (EDA) favours interaction energies for the systems containing the Eq isomer. However, when solvent effects are taken into account the systems containing the Ax isomer are again the most stable. This Ax isomer was found interacting by means of end-stacking with the GQ and surprisingly totally inside the non-canonical secondary structure, where all the ligands of the metal complex produce several weak interactions with the DNA structure. On the other hand, the Eq isomer prefers to interact from outside by means of intercalation in which the ancillary ligands have also some role in the interaction. Such features and comparison with the results regarding the interaction of the  $[\text{Mo}(\eta^3\text{-C}_3\text{H}_5)\text{Br}(\text{CO})_2(\text{phen})]$  metal complex with duplex DNA suggest that the  $[\text{Mo}(\eta^3\text{-C}_3\text{H}_5)\text{Br}(\text{CO})_2(\text{phen})]$  would have higher affinity and eventual selectivity for non-canonical DNA GQ structures.

## Introduction

During the last decades, cancer has been one of the most studied diseases. Unfortunately, it has also been one of the diseases with lowest clinical success rates, where improving and finding new drugs against it is still a current subject of study.<sup>1</sup>

One of the first effective drugs against cancer was the well-known cis-platin, reported by Rosenberg et al. in 1965.<sup>2</sup> However, its toxicity limits its use in humans. To overcome this problem, one step beyond was done with the non-covalent binding interacting ligands,<sup>3-5</sup> where the interaction is strong enough to interrupt certain key biological processes such as DNA transcription or replication, which directly affect the growth of tumoral cells. On the other hand, an alternative and innovative strategy that is being explored during the last years to overcome the abovementioned secondary effects of toxicity for people is the use of the non-canonical secondary DNA structures called G-quadruplexes (GQ), which may be used as specific targets.<sup>6,7</sup> GQ have been found at key points in the genome that directly relate it to cancer, such as telomeres or oncogene promoters<sup>8,9</sup> and their stabilisation is crucial for the disruption of the transcription and replication processes in DNA. In this sense, it must be said that even though there are different ways to stabilise GQ with ligands and other small molecules,<sup>10-12</sup> the use of small molecules not only stabilises GQ but also induces the formation of GQ around the small molecule.<sup>13</sup>

Most of the studied molecules that can interact with duplex DNA (dDNA) and GQ in a non-covalent way are planar organic

<sup>a</sup> CIC-nanoGUNE BRTA, Tolosa Hiribidea 76, E-20018, Donostia – San Sebastián, Euskadi, Spain; E-mail: [adria.gil.mestrs@csic.es](mailto:adria.gil.mestrs@csic.es); [adriaqilmestres@unizar.es](mailto:adriaqilmestres@unizar.es); [agmestres@fc.ul.pt](mailto:agmestres@fc.ul.pt)

<sup>b</sup> Polímero eta Material Aurreratuak: Fisika, Kimika eta Teknologia, Kimika Fakultatea, Euskal Herriko Unibertsitatea, UPV/EHU, 20080 Donostia, Euskadi, Spain.

<sup>c</sup> BioISI – Biosystems and Integrative Sciences Institute, Faculdade de Ciências, Universidade de Lisboa, Campo Grande, 1749-016, Lisboa, Portugal.

<sup>d</sup> Donostia International Physics Center (DIPC), P. K. 1072, 20080 Donostia, Euskadi, Spain.

<sup>e</sup> ARAID Foundation, Zaragoza, Spain.

<sup>f</sup> Departamento de Química Inorgánica, Instituto de Síntesis Química y Catálisis Homogénea (ISQCH) – Consejo Superior de Investigaciones Científicas (CSIC). Universidad de Zaragoza, c/ Pedro Cerbuna 12, 50009, Zaragoza, Spain

Electronic Supplementary Information (ESI) available: Scheme of the G-tetrad and G-quadruplex with labels in the atoms, relative energies and formation energies for the interaction between the  $[\text{Mo}(\eta^3\text{-C}_3\text{H}_5)\text{Br}(\text{CO})_2(\text{phen})]$  metal complex and the G-quadruplex, QTAIM topologies and values of the electronic density and Laplacian and energy density in each intermolecular BCP along with interatomic distances, and the cartesian coordinates of the four most stable optimised systems for each isomer, Ax and Eq, of the metal complex interacting with the G-quadruplex at LMKLL/DZDP level. See DOI: 10.1039/x0xx00000x

molecules,<sup>14</sup> such as phenanthroline (phen) and its derivatives.<sup>15–19</sup> In addition, many metal complexes, including phen and derivatives, have shown potential to inhibit the growth and survival of tumor cells, while being less toxic than cisplatin.<sup>20–22</sup> Alternatively, octahedral metal complexes containing planar ligands have also been investigated in a more reduced number of studies.<sup>23–29</sup> Among all the used metal elements molybdenum complexes have been very promising due to the fact that Mo is an essential trace in the human body, and it is characterised by its low toxicity.<sup>30</sup> Moreover, experimental studies demonstrated the efficacy of a molybdenum octahedral metal complex containing phen, [Mo( $\eta^3$ -C<sub>3</sub>H<sub>5</sub>)Br(CO)<sub>2</sub>(phen)], against different tumoral cell lines.<sup>31</sup>

GQ structures and its interaction with metal complexes have also been studied by computational methods.<sup>32</sup> Molecular dynamics (MD) simulations have been the most used computational methods to study GQ structures and their interactions. Indeed, different metal complexes have been studied, such as various Salphen- and Schiff-base metal complexes,<sup>33–36</sup> and their interaction with GQ or the interaction of GQ with metal complexes containing phen derivatives.<sup>37</sup> Moreover, regarding the use of MD simulations, it must be also highlighted the recent work of Giambaşu et al.<sup>38</sup> who combined the OL15 force field with 3D-RISM molecular solvation theory to create a predictive model for cation occupancy in GQ channels as a function of salt concentration. On the other hand, GQ have also been studied by means of QM/MM, both structural studies<sup>39,40</sup> and the interaction with ligands.<sup>41,42</sup> Nevertheless, studies analysing the interaction of such structures with metal complexes by means of QM/MM are scarce in the literature.<sup>43,44</sup> As an alternative to classical MD and QM/MM methods, a recent fully QM theoretical study on the interaction of this Mo phen-based metal complex with the dDNA was performed in our team by using linear-scaling DFT (LS-DFT) for a system involving the complex and a dDNA octamer (a system of more than 500 atoms).<sup>45</sup> Seminal works of Yang et al.<sup>46,47</sup> on the application of LS-QM methods to large biomolecules have been found in the bibliography. However, as far as we know, no studies are found in the literature in which the interaction of any metal complex with the whole non-canonical GQ secondary structure including not only DNA bases and cations but also the sugar and phosphate backbone has been studied at first principles QM level and because we already analysed the interaction of metal complexes with dDNA at LS-DFT level with success, we decided to study the interaction of the [Mo( $\eta^3$ -C<sub>3</sub>H<sub>5</sub>)Br(CO)<sub>2</sub>(phen)] octahedral metal complex with a non-canonical DNA GQ secondary structure at the same level of calculation with a system of ~1000 atoms.

Thus, in the present work, we will study the non-covalent interaction of two isomers, Equatorial (Eq) and Axial (Ax), of the [Mo( $\eta^3$ -C<sub>3</sub>H<sub>5</sub>)Br(CO)<sub>2</sub>(phen)] octahedral metal complex (Fig. 1) with the DNA GQ by means of first principles LS-DFT methods. That is, LS-DFT will be used for the first time to study the interaction of GQ with metal complexes by using the SIESTA software,<sup>48,49</sup> which is capable of performing DFT calculations for big biological systems of >1000 atoms. To study the nature

of the interaction we will use methods like the Quantum Theory of Atoms in Molecules (QTAIM),<sup>50</sup> Non-Covalent Interactions (NCI) index<sup>51,52</sup> and the Energy Decomposition Analysis (EDA).<sup>53</sup> In addition, at the end of the Results and Discussion section, a comparison of the interaction of our [Mo( $\eta^3$ -C<sub>3</sub>H<sub>5</sub>)Br(CO)<sub>2</sub>(phen)] metal complex with GQ and dDNA structures will be performed in order to gain insight about the affinities and the selectivity of any isomer of this metal complex for dDNA vs. GQ substrate. These studies on the affinities and selectivity of small molecules with canonical dDNA and non-canonical structures of DNA like GQ structures is a current topic of research in the bibliography.<sup>32,54</sup>

## Computational Details

In order to build our system we used a four stranded parallel GQ as starting point structure from Protein Data Bank (PDBID: 2jwq).<sup>55</sup> This structure has two quinacridine-based ligand (MMQ) units, each bounded by means of the end-stacking mode of interaction at both sides of the GQ. In order to predict the binding of the two isomers, Ax and Eq, of the [Mo( $\eta^3$ -C<sub>3</sub>H<sub>5</sub>)Br(CO)<sub>2</sub>(phen)] metal complex with GQ coming from the 2jwq structure molecular docking was carried out as we describe in the following lines. The MMQ ligands were removed from the original structure of the PDB, which leaves a gap at the end-stacking of the GQ where the [Mo( $\eta^3$ -C<sub>3</sub>H<sub>5</sub>)Br(CO)<sub>2</sub>(phen)] metal complex could potentially be introduced in the docking computations. The HEX v.8.0.0 package<sup>56</sup> was used for the docking calculations considering, in general, the keywords by default and the manual recommendations for the DNA structure interacting with the metal complex. Nevertheless, we changed some of the default parameters in order to have different sets of conformations for each isomer of the [Mo( $\eta^3$ -C<sub>3</sub>H<sub>5</sub>)Br(CO)<sub>2</sub>(phen)] metal complex. That is, a) in a first docking calculation the *Correlation Type* was changed to Shape + Electro to take into account not only the surface shape, but also the electrostatic charge distribution, whereas the *Post Processing* was changed to OPLS Minimisation; b) in the second docking calculations we added the Decoy As the Reference State (DARS)<sup>57</sup> and we used the *Correlation Type* as Shape + Electro + DARS, while the *Post Processing* was changed to DARS Minimisation; c) the third docking calculations were carried out with the parameters by default, that is, *Correlation Type* as Shape and no *Post Processing*. In all cases the number of *Solutions* was modified to 50000 and the *Final Search* parameter was changed to 30 (because the initial PDB structure had high resolution). In order to group similar structures found in the docking calculation, the structures were organised in 100 clusters, with a cluster window of 50 and a threshold root mean square (RMS) of 1.5. The rest of parameters of the clustering control panel were kept as the default. These different docking calculations were performed for each isomer, Ax and Eq, of the [Mo( $\eta^3$ -C<sub>3</sub>H<sub>5</sub>)Br(CO)<sub>2</sub>(phen)] metal complex and the lowest-energy systems from the docking calculations interacting through end-stacking and intercalation between DNA bases with the GQ were used as starting points for the LS-DFT optimisations. We assume that this sampling method with

docking and subsequent optimisations via LS-DFT will produce structures very close to the initial structure found with docking and will be dependent of the scoring function of HEX. Nevertheless, since we considered up to 3 different docking calculations differing from the abovementioned parameters and in each docking calculation we found that the  $[\text{Mo}(\eta^3\text{-C}_3\text{H}_5)\text{Br}(\text{CO})_2(\text{phen})]$  metal complex was interacting in very different regions of the GQ (end-stacking, intercalation, groove binding, etc.), we consider that the most important regions of interaction of the metal complex with the GQ have been explored, at least within the possibilities given by the scoring function of HEX. The obtained systems from docking, a total of 55 structures, were neutralised by adding  $\text{K}^+$  close to phosphate groups at a distance of 2.7 Å, and two additional  $\text{K}^+$  were also added at the centre of the GQ in the same way as suggested in the work of Hounsou et al.<sup>55</sup> That is, each  $\text{K}^+$  cation was coordinated to eight  $\text{O}_6$  (see Figure S1) from the G-tetrads of guanines, resulting in a +2 charged system. For the LS-DFT optimisations of the whole system with 966 atoms SIESTA 4.1-b3 software<sup>48,49</sup> was used with the LMKLL<sup>58</sup> van der Waals functional, which includes dispersion corrections, being highly appropriate to characterise weak forces between the ligand and DNA. This functional was found to perform excellently for geometrical parameters and energetics of GQ.<sup>59</sup> The system was included in a unit cell with a cell vector, in Å, of (60.0, 60.0, 60.0) and only the  $\Gamma$   $k$ -point was considered in the calculation. In order to achieve good geometries, the modified Broyden algorithm was used,<sup>60</sup> SCF was accelerated with the Pulay method,<sup>61,62</sup> keeping the history of 4 past matrices, the density matrix mixing weight was set to 0.005, 30 meV for the energy shift and a 150 Ry mesh cut off. We also considered the SCF tolerance of  $1 \times 10^{-5}$  eV and we set the max force tolerance to 0.1 eV/Å. Double- $\zeta$  plus double polarisation (DZDP) numerical basis sets<sup>63</sup> were used in which core electrons were substituted by norm-conserving pseudopotentials,<sup>64,65</sup> optimised for each element of the system with the ATOM package included in SIESTA. No solvent effects were considered for SIESTA optimisations but they will be taken into account in subsequent calculations on the interaction energy. For a better understanding of the nature of the interaction for the  $[\text{Mo}(\eta^3\text{-C}_3\text{H}_5)\text{Br}(\text{CO})_2(\text{phen})]$  complex with the DNA GQ we carried out the EDA calculations for the five most stable structures of each isomer obtained from the previous optimisations. This EDA was carried out by using the ADF software<sup>66-68</sup> In the EDA the interaction energy ( $\Delta E_{\text{int}}$ ) between fragments (DNA and ligand) is split into different energy terms following the Morokuma energy decomposition method<sup>69</sup> as follows:

$$\Delta E_{\text{int}} = \Delta E_{\text{elstat}} + \Delta E_{\text{Pauli}} + \Delta E_{\text{orb}} + (\Delta E_{\text{disp}}) \quad (1)$$

Moreover, we may define the steric contributions as:<sup>70</sup>

$$\Delta E_{\text{steric}} = \Delta E_{\text{elstat}} + \Delta E_{\text{Pauli}} \quad (2)$$

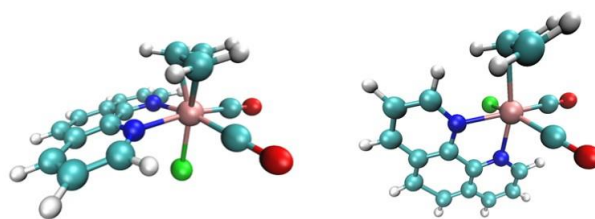


**Fig. 1.** Eq (left) and Ax (right) isomers of the  $[\text{Mo}(\eta^3\text{-C}_3\text{H}_5)\text{Br}(\text{CO})_2(\text{phen})]$  metal complex. The Eq isomer is the most stable in the solid state but in aqueous solution both isomers Eq and Ax are fluxional.

As stated by Hopffgarten and Frenking,<sup>53</sup> if an explicit correction term for dispersion is used, the EDA results remain unchanged and the dispersion correction appears as a  $\Delta E_{\text{disp}}$  extra term. In contrast, if the dispersion contribution is part of the functional, it will change the EDA results by weakening the  $\Delta E_{\text{Pauli}}$  repulsive contribution. We already compared the EDA's for intercalated systems by using functionals with the explicit and implicit  $\Delta E_{\text{disp}}$  contributions, and we obtained similar results for all the compared final  $\Delta E_{\text{int}}$  interaction energies.<sup>15-17</sup> However, because it is more useful to have an explicit contribution for the  $\Delta E_{\text{disp}}$  term in the EDA, the calculations were performed with the B3LYP-D3 functional,<sup>71,72</sup> which includes Grimme's dispersion corrections<sup>73</sup> as the explicit term for  $\Delta E_{\text{disp}}$ . We used two kinds of basis sets with different size in order to see how the EDA is affected by the size of the basis set, that is, uncontracted polarised double- $\zeta$  and triple- $\zeta$  basis sets of Slater type orbitals (DZP and TZP, respectively). For the former no frozen core approach was used, whereas for the latter a medium frozen core approximation was employed because of the size of the system (966 atoms). Relativistic effects were treated with the Zero Order Regular Approximation (ZORA) Hamiltonian.<sup>74-79</sup> Solvent effects were taken into account by using COSMO solvation model as implemented in ADF.<sup>80</sup> As far as we know, there should not be reactive processes involving the solvent and we believe that labile interactions of the hydrogen bonding produced between the solvent (water) and the structures studied in this work (GQ interacting with metal complexes) may be averaged automatically through such continuum model.<sup>81</sup> In order to gain insight into the nature of the interaction between the Mo complex including phen and the DNA GQ, the topology of the electron density was analysed with QTAIM.<sup>50</sup> The wave functions used for these QTAIM calculations were computed with Gaussian16<sup>82</sup> at M11L/6-31+G(d,p) level of theory with the exception of the Mo atom, where we used the LANL2DZ effective core potential and the associated basis set<sup>83</sup> supplemented with f-polarisation functions.<sup>84</sup> It must be said that in order to avoid the generation of huge wave functions for these systems of 966 atoms, the structure of the GQ interacting with the metal complex was trimmed by keeping the regions in which the Mo complex produces the so-called Bond Critical Points (BCP's)<sup>50</sup> with the GQ and removing the rest of atoms. The AIMALL software<sup>85</sup> was used to carry out such QTAIM analyses. Moreover, the topology of the electronic density ( $\rho$ )

was analysed to explore the Non-Covalent Interaction (NCI) index developed by Johnson et al.<sup>51</sup> Such NCI analyses were also performed with the AIMALL software.

## Results and Discussion

### Geometries and energetics

Fig. 2 shows the most stable optimised geometrical structures for the Eq and Ax isomers of the  $[\text{Mo}(\eta^3\text{-C}_3\text{H}_5)\text{Br}(\text{CO})_2(\text{phen})]$  complex when interacting with the DNA GQ through end-stacking or via intercalation between base pairs (bps) along with the relative energies (formation energies are depicted in Table S1 of the ESI). It must be said that whereas all most stable Ax isomers interact via end-stacking with the GQ and the systems are quite similar with the Ax isomer localised inside the non-canonical DNA secondary structure, in the case of the Eq isomers there was not any system in which the Eq isomer of the  $[\text{Mo}(\eta^3\text{-C}_3\text{H}_5)\text{Br}(\text{CO})_2(\text{phen})]$  metal complex was interacting via end-stacking and the conformational diversity is richer than for the Ax isomer. Indeed, for the most stable systems including the Eq isomer we found all the metal complexes interacting with the DNA GQ from outside; three intercalating the phen ligand between the bases of the GQ, one interacting with the GQ through the Br atom and one interacting with the GQ by means of the allyl ligand.

Looking at the relative energies (see Fig. 2) and formation energies ( $\Delta E_{\text{form}}$ , see Table S1 of the ESI), the most stable systems including the Ax isomer have the metal complex forming the so-called end-stacking binding mode. In this sense, more surprising is the fact that the metal complex is located inside the non-canonical secondary structure of the DNA, completely surrounded by not only the G-tetrads of the GQ but also the consecutive adenine tetrads. It means either that the DNA has to unfold itself to allocate the metal complex in that position and when folding back it traps the metal complex or that the metal complex promotes the folding of such non-canonical DNA secondary structures around it. On the other hand, the most stable Ax isomers have the Br atom facing opposite to the G-tetrads therefore, moving away from the generated ion-channel, where the  $\text{O}_6$  atoms of guanine bases (see Fig. S1 of the ESI) form a high electron density concentration, which is an ideal spot to place positively charged metal ions as the  $\text{K}^+$  or other alkaline cations but not electronegative atoms such as Br. Finally, it must be said that in all cases the phen ligand is parallel to the G-tetrads, which suggests the presence of  $\pi$ - $\pi$  interactions between phen and the closer G-tetrad.

On the other hand, none of the most stable systems including the Eq isomer places it inside the DNA secondary structure. Indeed, the Eq isomer of the  $[\text{Mo}(\eta^3\text{-C}_3\text{H}_5)\text{Br}(\text{CO})_2(\text{phen})]$  metal complex is more stable either intercalating the bases of DNA from outside or interacting through the allyl or the halogen ligand with the DNA. This is an interesting result because it opens the door to the possibility of modulation of the interaction not only by substitution of the phen planar ligand but also by substitution of the ancillary ligands, which would

have significant role in the interaction of the Eq isomer with the DNA GQ.

EDA was performed to determine the different contributions to the  $\Delta E_{\text{int}}$  between the complex and the GQ and to rationalise the order of stability of the structures (see Fig. 3). In the case of Eq systems the most negative value for the  $\Delta E_{\text{int}}$  was given by the Eq1 system, coming in hand with the relative and formation energies obtained before for the same Eq system (see Fig. 2 and Table S1 of the ESI). Nevertheless, now, the  $\Delta E_{\text{int}}$  for the Eq systems results more negative than for the Ax systems as a general trend, with exception of Eq3 system. On the other hand, it must be said that for Ax systems, the most negative  $\Delta E_{\text{int}}$  does not correspond to the Ax1 system, which had the lowest relative energy and most negative  $\Delta E_{\text{form}}$ , but to the Ax4 structure, having the Ax1 the second most negative  $\Delta E_{\text{int}}$  and only differing by  $1.9 \text{ kcal mol}^{-1}$  from the  $\Delta E_{\text{int}}$  of Ax4. It must be remembered that for the calculation of the  $\Delta E_{\text{int}}$  the relaxation or preparation energy<sup>50</sup> is not considered. Taking into account that all the 4 lowest energy Ax structures include the  $[\text{Mo}(\eta^3\text{-C}_3\text{H}_5)\text{Br}(\text{CO})_2(\text{phen})]$  metal complex interacting via end-stacking with the GQ inside the DNA secondary structure in a similar way, we attribute such differences mainly to the relaxation / preparation energy and to a lesser extent to the different level of calculation (LMKLL/DZDP with SIESTA vs. B3LYP-D3/TZP with ADF). On the other hand, all the contributions to the  $\Delta E_{\text{int}}$  become more important for the Ax structures than for the Eq systems with the exception of  $\Delta E_{\text{orb}}$ . This is not surprising since for the Ax systems the metal complex is completely surrounded by the atoms of the non-canonical DNA secondary structure, which leads to stronger interactions. As a result, we have higher repulsive ( $\Delta E_{\text{Pauli}}$ ) and attractive ( $\Delta E_{\text{elstat}}$  and  $\Delta E_{\text{disp}}$ ) contributions. At this point it must be highlighted that the  $\Delta E_{\text{disp}}$  rules the nature of the interaction for the Ax systems, whereas in the case of the Eq structures  $\Delta E_{\text{elstat}}$  and  $\Delta E_{\text{disp}}$  contributions have both a similar important role, as a general trend, to define the nature of the interaction. The  $\Delta E_{\text{steric}}$  term, consisting of the sum of the repulsive  $\Delta E_{\text{Pauli}}$  and the attractive  $\Delta E_{\text{elstat}}$  contribution terms (Eq. 2) is very similar when comparing to the systems of the same family (Eq or Ax). In the case of Ax systems, with the exception of Ax2 ( $47.3 \text{ kcal mol}^{-1}$ ),  $\Delta E_{\text{steric}}$  ranges from  $78.7 \text{ kcal mol}^{-1}$  to  $81.1 \text{ kcal mol}^{-1}$ , with a difference of only  $2.4 \text{ kcal mol}^{-1}$ . For the Eq systems, with the exception of Eq3 ( $46.6 \text{ kcal mol}^{-1}$ ), the  $\Delta E_{\text{steric}}$  has even lower differences among the systems, and it ranges from  $22.0$  to  $22.4 \text{ kcal mol}^{-1}$ , which is a difference of less than  $0.5 \text{ kcal mol}^{-1}$ . Again, as stated above, we may attribute these higher values of  $\Delta E_{\text{steric}}$  for the Ax systems when comparing to the Eq systems to the fact that in the Ax systems the metal complex is completely inside the cavity of the non-canonical DNA secondary structure not only interacting through the end-stacking mode with the GQ but also interacting with the subsequent adenine tetrads. In such interaction, the Ax isomer of the  $[\text{Mo}(\eta^3\text{-C}_3\text{H}_5)\text{Br}(\text{CO})_2(\text{phen})]$  metal complex is surrounded by many atoms, which makes the  $\Delta E_{\text{steric}}$  term higher than those obtained for the Eq systems, which interacts with less atoms as a general trend. The values obtained for the  $\Delta E_{\text{disp}}$  are also interesting. That is, all the values obtained for the  $\Delta E_{\text{disp}}$  term are more negative for the Ax structures than for the

Eq systems (an average value of  $\sim 30$  kcal mol $^{-1}$  more negative). The more negative values of  $\Delta E_{disp}$  for the Ax isomer are in agreement with the results obtained with the QTAIM and NCI

analyses discussed below (Fig. 4 and Fig. 5) for which more weak interactions related to dispersion forces are appreciated.

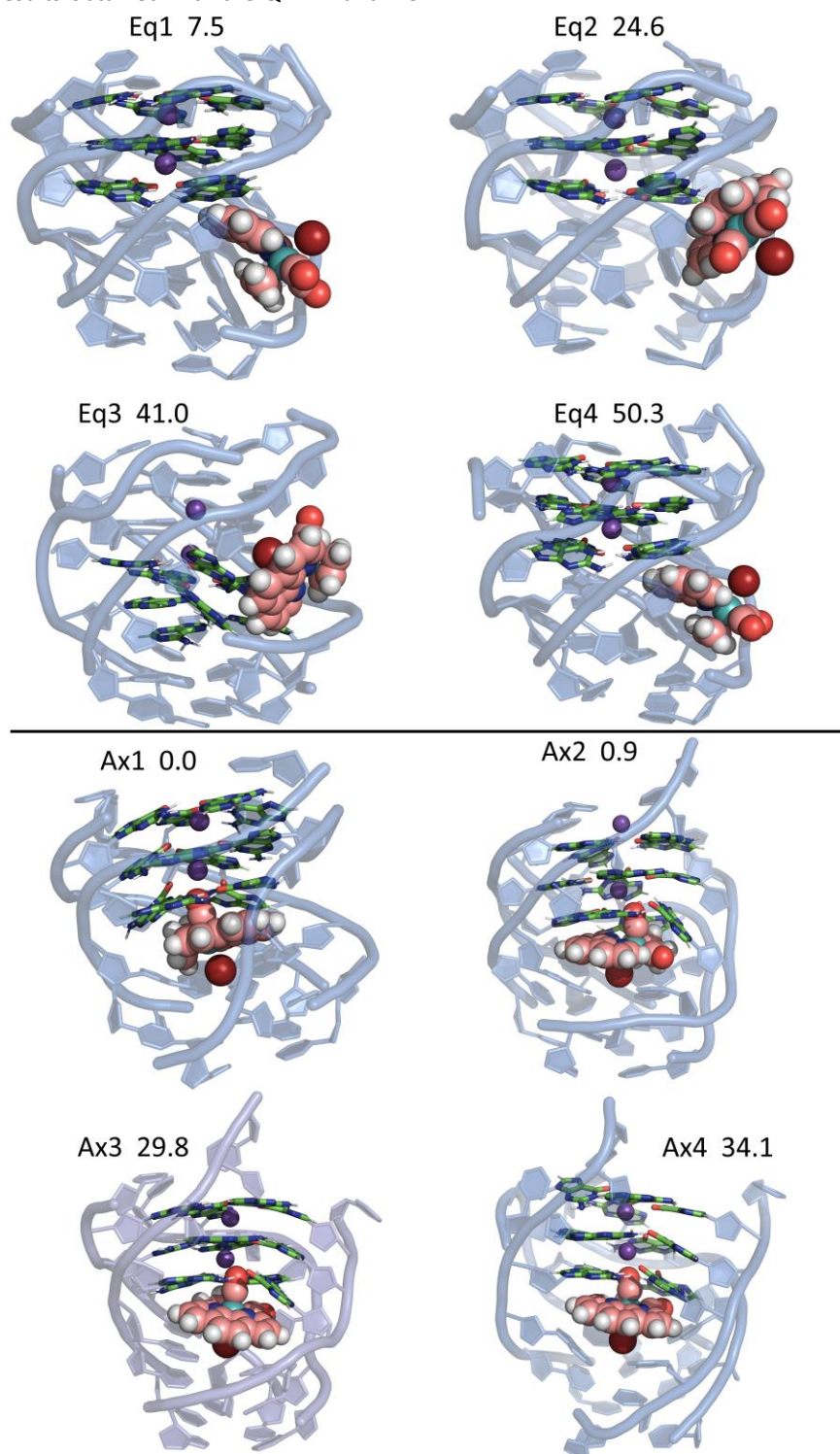


**Fig 2.** Most stable optimised structures for the interaction between Eq (top) and Ax (bottom) metal complex with the studied GQ at LMKLL/DZDP level along with the relative energy differences in kcal mol $^{-1}$  taking the most stable Ax1 structure as the reference.

In any case, it must be highlighted that in all cases the rest of the ligands have an important role producing other weak interactions with the non-canonical DNA structure and reinforcing the interaction. In this sense, it must be highlighted that the ancillary ligands play a most important role and

produce more weak interactions in the Ax systems than in the Eq structure as we will see below in the section corresponding to the analysis of the weak interactions. On the other hand, the phen ligand has the most significant differences depending on if it is interacting from outside or through the end-stacking

mode of interaction with the GQ inside the cavity of the non-canonical secondary DNA structure.

In order to analyse the effect of the size of the basis set, we also carried out the EDA calculations with a double- $\zeta$  basis set plus polarisation (DZP). Obtained energies are depicted in Table S2 of the ESI. It is observed that as a general trend the  $\Delta E_{int}$  values obtained with the DZP are more negative. That is,  $\sim 30\%$  more negative in the case of the Eq systems, whereas for the Ax systems the difference is even more considerable (50 – 60% more negative) when comparing to the results obtained with the TZP basis set. Actually, when using the DZP basis set in the EDA, the  $\Delta E_{int}$  energies of the Eq and Ax systems are more similar among them, whereas when the TZP basis set is used, a clear general trend appeared where the Eq systems had more negative  $\Delta E_{int}$  energies than the Ax systems. In addition, in the case of Ax systems, when computing the EDA's and  $\Delta E_{int}$  with the DZP basis set, the system with more negative  $\Delta E_{int}$  was Ax1, while for the computations with the TZP basis set it was the Ax4 structure. In the case of the Eq systems the order was not changed and Eq1 has still is the most negative  $\Delta E_{int}$ . In the case of the TZP basis set, the most important attractive contribution is  $\Delta E_{disp}$  for Ax systems, whereas for Eq systems the values of  $\Delta E_{elstat}$  and  $\Delta E_{disp}$  are similar. In contrast, for the EDA's

performed with the DZP, in all systems, Eq and Ax, the most important attractive contribution is in general  $\Delta E_{elstat}$ , with the exception of Ax4 and Eq3 structures, but the difference with respect  $\Delta E_{disp}$  is now lower than when comparing  $\Delta E_{disp}$  and  $\Delta E_{elstat}$  of the Ax systems in the calculations with the TZP basis set. It is also interesting to observe how in the case of the DZP the attractive interaction  $\Delta E_{orb}$  is also more negative than when the EDA is carried out with the TZP basis set ( $\sim 10$  kcal mol<sup>-1</sup> more negative in the case of the Eq systems and  $\sim 20$  kcal mol<sup>-1</sup> more negative for the Ax structures as a general trend), which is in agreement with the trends found in the bibliography stating that medium-size basis sets overestimate the charge-transfer energy associated to  $\Delta E_{orb}$ .<sup>19,86,87</sup> Finally, the  $\Delta E_{Pauli}$  repulsive contribution is more positive, as a general trend, when the EDA is performed with the DZP basis set than when it is carried out with the TZP basis set. Taking all these considerations into account, the use of a TZP basis set is justified for the correct description of the energy contributions in the EDA and the presentation of the results for this kind of systems including  $\sim 1000$  atoms. Even though the calculations with the TZP basis set requires more computational resources in terms of memory, disk, computing-time, etc. we were able to carry out such computations for systems with  $\sim 1000$  atoms in our local cluster.

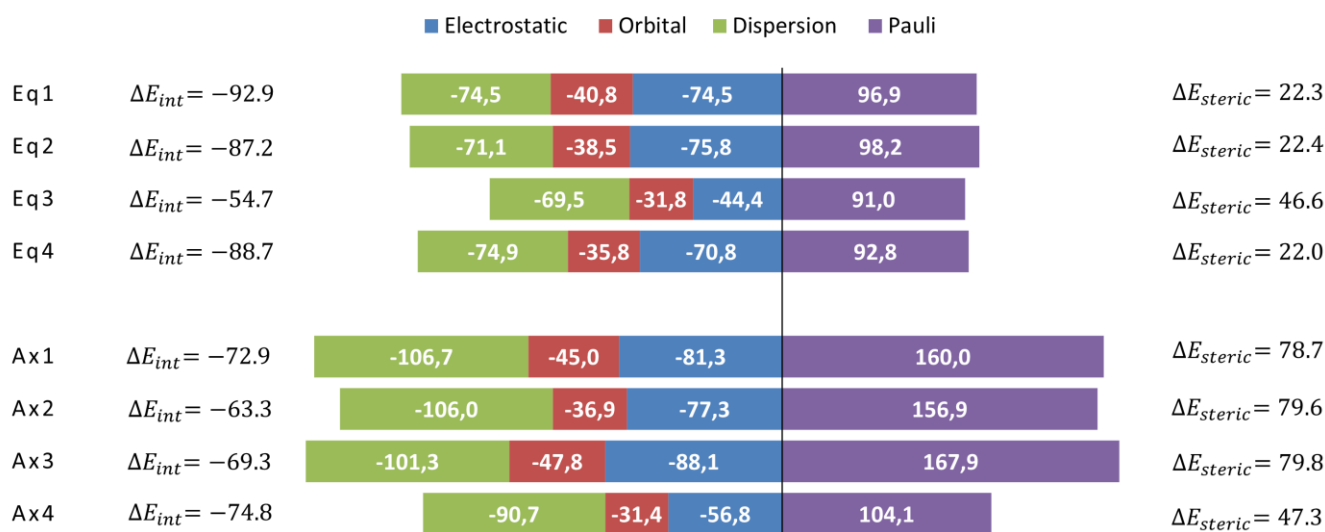


**Fig 3.** Cumulative bar diagram of the different contributions in the EDA at the B3LYP-D3/TZP level. The total interaction energy is written in the second column and the so-called steric energy in the last column. All the energy contributions and the total interaction energy are given in kcal mol<sup>-1</sup>.

### Solvent effects

To gain more insight into the solvent effects (water) in the studied processes, the desolvation penalty ( $\Delta E_{solv}$ ) of the total interaction energy ( $\Delta E_{int}$ ) was calculated by means of the COSMO continuum model.<sup>80</sup> Table 1 collects the solvation energies for the four most stable systems for each isomer of the [Mo( $\eta^3$ -C<sub>3</sub>H<sub>5</sub>)Br(CO)<sub>2</sub>(phen)] complex interacting with the GQ DNA non-canonical secondary structure addressed in this work. We observe that for such interaction the trends in the stabilisation of the systems may change when the solvent effects are included, as observed in previous works, in which phen derivatives interacted with dDNA.<sup>17,88</sup> Indeed, as was observed above in the EDA, the  $\Delta E_{int}$  interaction energy

between the studied GQ non-canonical DNA secondary structure and the [Mo( $\eta^3$ -C<sub>3</sub>H<sub>5</sub>)Br(CO)<sub>2</sub>(phen)] metal complex is clearly more negative for Eq systems than in the case of Ax structures when only the intrinsic contributions to the interaction were taken into account ( $\Delta E_{Pauli}$ ,  $\Delta E_{orb}$ ,  $\Delta E_{elstat}$ , and  $\Delta E_{disp}$ ). However, when we consider  $\Delta E_{aq}$ , defined as  $\Delta E_{aq} = \Delta E_{int} + \Delta E_{solv}$  with  $\Delta E_{solv} = E_{solv}(\text{total system}) - E_{solv}(\text{GQ}) - E_{solv}(\text{metal complex})$ , the values of the  $\Delta E_{aq}$  are more negative for the systems including the Ax isomer, being Ax4 with  $\Delta E_{aq} = -46.0$  kcal mol<sup>-1</sup> the most stable system. This behaviour arises from the important  $\Delta E_{solv}$  penalty obtained for the systems containing Eq complexes interacting from outside with the non-canonical DNA secondary structure (from 37 to 62 kcal mol<sup>-1</sup>),

which is higher than the values for the systems containing the Ax isomer inside the non-canonical DNA secondary structure (from 27 to 35 kcal mol<sup>-1</sup>). This  $\Delta E_{solv}$  penalty may reverse the order of stability of the systems, and thus, the inclusion of solvent effects becomes crucial for the final stabilisation of the studied structures. Thus, consideration of solvent effects lead to more negative values for  $\Delta E_{aq}$  in the systems containing the Ax isomer of the  $[\text{Mo}(\eta^3\text{-C}_3\text{H}_5)\text{Br}(\text{CO})_2(\text{phen})]$  metal complex in contrast to the most negative  $\Delta E_{int}$  energies obtained for the systems with the Eq isomer when solvation effects were not taken into account.

### Analysis of the weak interactions

QTAIM topologies and the NCI index analysis provide insight into the weak interactions between the  $[\text{Mo}(\eta^3\text{-C}_3\text{H}_5)\text{Br}(\text{CO})_2(\text{phen})]$  complex and the GQ. The QTAIM topologies and the values of  $\rho$  on the BCPs for the most stable studied structures are depicted in Fig. S2-S9 and Tables S3-S10 of the ESI. In order to show a clearer picture only the

surrounding environment of the metal complex was plotted in the figure while the remaining structure of the non-canonical DNA system was trimmed. Moreover, the NCI isosurfaces were only plotted in the areas located between the metal complex and the GQ non-canonical DNA structure, avoiding the NCI isosurfaces that appear between sugar and phosphate groups that would overload the picture. The gradient isosurfaces are coloured according to the values of  $\text{sign}(\lambda_2)\rho$ . Isosurfaces with blue and pale green are associated to stabilising interactions (negative values). On the other hand, yellow and red isosurfaces correspond to repulsive interactions (positive values). Very weak interactions with values close to zero are depicted in green. Fig. 4 and Fig. 5 show the NCI results for the Ax4 and Eq4 systems, respectively, which were the arrangements with more negative interaction energy for each isomer, Ax and Eq, of the  $[\text{Mo}(\eta^3\text{-C}_3\text{H}_5)\text{Br}(\text{CO})_2(\text{phen})]$  complex when it is interacting with the DNA GQ after the consideration of solvent effects (see  $\Delta E_{aq}$  values in Table 1). All the studied structures including the NCI analysis are found in the ESI (Fig. S10-S17).

**Table 1.** Contributions of the solvation energies for the studied systems at B3LYP-D3/TZP level using COSMO approach. All the energies are given in kcal mol<sup>-1</sup>. The final energy in solution ( $\Delta E_{aq}$ ) corresponds to the sum of  $\Delta E_{int}$  and  $\Delta E_{solv}$  terms ( $\Delta E_{aq} = \Delta E_{int} + \Delta E_{solv}$ ).

System	$E_{solv}$ (total system)	$E_{solv}$ (metal complex)	$E_{solv}$ (GQ)	$\Delta E_{solv}$	$\Delta E_{int}$	$\Delta E_{aq}$
Ax1	-457.0	-25.1	-463.0	31.0	-72.9	-41.9
Ax2	-424.0	-22.7	-428.9	27.6	-63.3	-35.7
Ax5	-456.1	-23.5	-467.4	34.9	-69.3	-34.5
Ax3	-471.2	-22.5	-477.5	28.8	-74.8	-46.0
Eq1	-463.3	-30.1	-494.1	60.9	-92.9	-32.0
Eq2	-478.4	-29.4	-510.7	61.7	-87.2	-25.5
Eq3	-498.2	-22.8	-512.6	37.2	-54.7	-17.5
Eq4	-506.3	-29.1	-531.2	54.0	-88.7	-34.6

For the Ax4 arrangement, as we have observed above, the coordination complex is fully inserted into the DNA non-canonical secondary structure and at the same time the phen planar aromatic ligand is horizontal with respect to the G-tetrads, whereas the ancillary ligands are confronted to such bases. This stable arrangement can be explained by means of the interactions presented in the NCI analysis. Firstly, the Br atom interacts with different bases because it is located in the ion-channel of the GQ showing isosurfaces mapped in pale blue, which indicates stabilising interactions. The same situation is found for the CO group opposite to the Br atom that is also located at the centre of the structure. This CO group interacts with different atoms of the G-tetrad and also with the cation located at the centre of the GQ. One of these interactions corresponds to a H atom of a G-tetrad and presents a high negative value for the  $\text{sign}(\lambda_2)\rho$ . Regarding the allyl group, a considerable region of interaction is shown, which corresponds to  $\pi$ - $\pi$  interactions with the nearby base plane. All these results indicate that the ancillary ligands play an important role in the interaction. On the other hand, the surrounding area of the phen ligand presents large isosurfaces corresponding to  $\pi$ - $\pi$  stacking interactions between the aromatic moieties. The main conclusion that arises from these results is that when the interaction of the  $[\text{Mo}(\eta^3\text{-C}_3\text{H}_5)\text{Br}(\text{CO})_2(\text{phen})]$  metal complex

and the non-canonical GQ DNA structure takes place from inside, both, the Br atom and the opposite CO group interact with the polar groups of the confronted bases. These contributions to the stabilisation are noteworthy due to the negative values for  $\text{sign}(\lambda_2)\rho$ , which show pale blue isosurfaces. The remaining isosurfaces correspond to the surrounding areas of the phen ligand and such interactions correspond mainly to the  $\pi$ - $\pi$  stacking of the phen ligand with the aromatic moieties of the G-tetrads. Moreover, the H atoms of phen show CH/ $n$  weak interactions that have been previously described in DNA ring models of phen derivatives interacting with dDNA.<sup>18,88</sup> In the case of Eq systems, the most negative  $\Delta E_{aq}$  energy has been found for the Eq4 system. In this geometrical arrangement the phen ligand of the  $[\text{Mo}(\eta^3\text{-C}_3\text{H}_5)\text{Br}(\text{CO})_2(\text{phen})]$  metal complex is intercalated between tetrads, while the ancillary ligands (Br, allyl and CO groups) remain in the outer part of the non-canonical GQ DNA secondary structure, being closer to the sugar and phosphate backbone. It is observed in Fig. 5 that the allyl group presents stabilising interactions with the O atoms belonging to the phosphate groups with a considerable negative value for  $\text{sign}(\lambda_2)\rho$  (pale blue). It must be said that the CO groups does not interact with any atom of the non-canonical GQ DNA secondary structure but with K cations that are placed in the surrounding areas of the sugar and phosphate backbone.

On the other hand, it is noteworthy to say that for this arrangement the Br atom is located outside of the GQ and it does not interact with any atom of the surrounding structures being only exposed to the solvation media. Finally, regarding phen, as a planar ligand, it is intercalated between the guanine and adenine tetrads. Such intercalation also yields the corresponding  $\pi$ - $\pi$  interactions and the CH/ $n$  interactions found previously for the Ax4 system.

### Discussion

The main remark arising from the previous analysis is the strong influence of the location of the interaction mode, with a clear difference when interacting between tetrads from inside or

interacting from outside of the non-canonical DNA secondary structure. When the ligand is interacting through end-stacking with the GQ totally inside the non-canonical DNA secondary structure, most of the interactions are produced with the bases of the DNA involving both, phen and the ancillary ligands. On the other hand, when the metal complex is interacting from outside of the non-canonical DNA secondary structure less  $\pi$ - $\pi$  interactions are found and the ancillary ligands interact mostly with the sugar and phosphate backbone. The results coming from the QTAIM and NCI analysis are in agreement with the EDA results. Our analysis may also be applied to explain the binding affinity and selectivity of the  $[\text{Mo}(\eta^3\text{-C}_3\text{H}_5)\text{Br}(\text{CO})_2(\text{phen})]$  for GQ vs. dDNA as we will see afterwards.

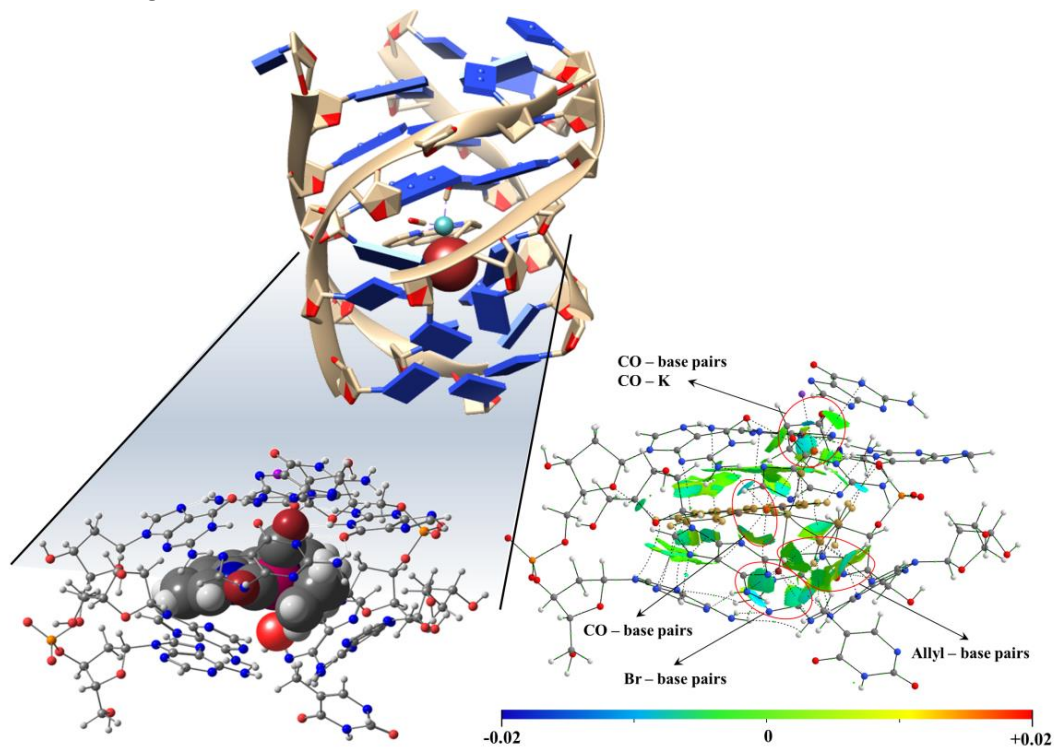
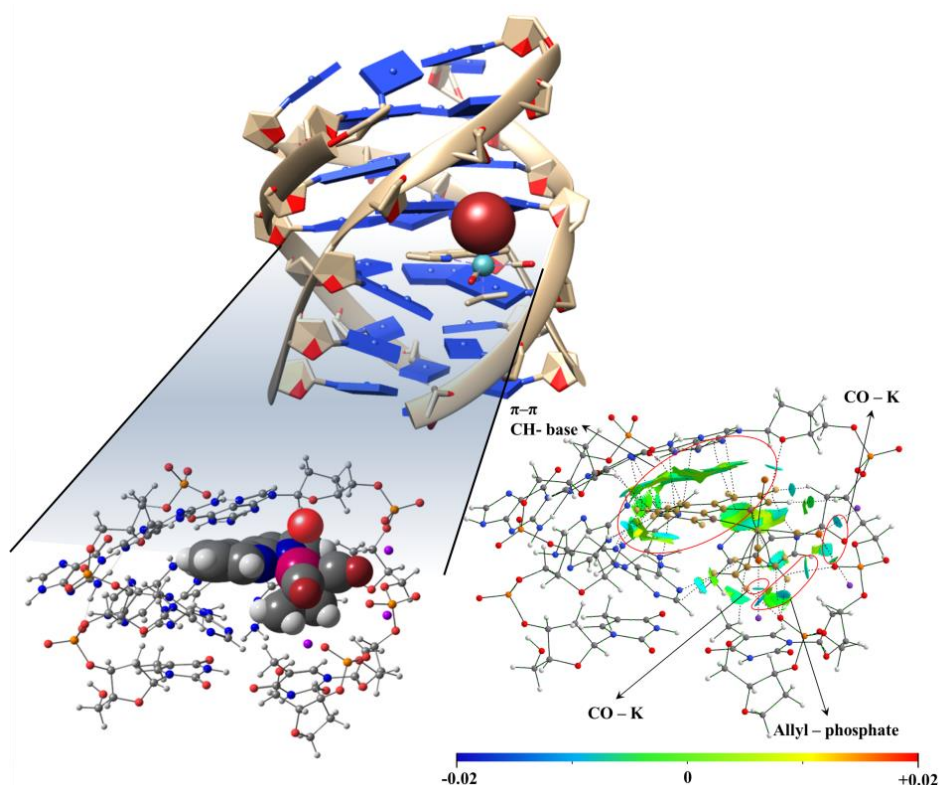


Fig 4. NCI plot with gradient isosurfaces ( $s = 0.5$  au) computed for the considered trimmed structure of Ax4.



**Fig 5.** NCI plot with gradient isosurfaces ( $s = 0.5$  au) computed for the considered trimmed structure of Eq4.

Looking at the formation energies of the  $[\text{Mo}(\eta^3\text{-C}_3\text{H}_5)\text{Br}(\text{CO})_2(\text{phen})]$  metal complex when interacting with the GQ, the energy difference between the binding mode achieved by each isomer, Ax and Eq, for the most stable systems is not really high. On the other hand, when considering the interaction energies  $\Delta E_{int}$  and  $\Delta E_{aq}$  the results are very different depending on whether solvent effects are or not are taken into account. That is,  $\Delta E_{int}$  is more negative when the Eq isomer of the  $[\text{Mo}(\eta^3\text{-C}_3\text{H}_5)\text{Br}(\text{CO})_2(\text{phen})]$  complex is intercalating from outside, whereas  $\Delta E_{aq}$  is more negative when the Ax isomer is interacting through end-stacking totally inside of the GQ DNA secondary structure. In this sense, it must be also said that this result regarding to the interaction of this octahedral metal complex totally inside the non-canonical DNA secondary structure is an outstanding result considering that in the literature no results were found in which octahedral metal complexes were interacting with the GQ totally inside the non-canonical secondary structure of the DNA.

The analysis based on the NCI and QTAIM shows that, end-stacking of the Ax complex with the DNA GQ should be favoured owing to the larger number of weak interactions than intercalation from outside the non-canonical DNA GQ secondary structure or any other interaction from outside. In the case of the Ax systems, the average value of weak interactions for the four most stable structures is 36 with an average accumulated  $\rho$  value (summation of the individual values of  $\rho$ ) of 0.30 au (see Tables S7-S10), whereas for the Eq systems the average of weak interactions is 33 with an average accumulated  $\rho$  value of 0.24 au (see Tables S3-S6). Even more, for each isomer, Ax and Eq of the  $[\text{Mo}(\eta^3\text{-C}_3\text{H}_5)\text{Br}(\text{CO})_2(\text{phen})]$  metal complex interacting with the GQ, the systems that

showed the highest number of weak interactions in the QTAIM and NCI analyses coincides with the system having the most negative formation energies. In the case of the Ax systems the lowest energy interacting structure is Ax1 (see Table S1 of the ESI), which shows 42 weak interactions (see Fig. S6 and Table S7 of the ESI). On the other hand, the most stable Eq interacting structure is the Eq1 system, which shows 36 weak interactions (see Fig. S2 and Table S3 of the ESI). The different number of weak interactions between the  $[\text{Mo}(\eta^3\text{-C}_3\text{H}_5)\text{Br}(\text{CO})_2(\text{phen})]$  complex and the GQ may be also appreciated in the NCI plots (see Fig. 4 and 5 of the manuscript and Fig. S10 – S17 of the ESI). The Ax isomer, which interacts by means of end-stacking between the tetrads and it is totally surrounded by DNA atoms has an extended green surface, which represents  $\pi$ - $\pi$  stacking interactions, whereas all the ancillary ligands are also taking some role in the interaction, all of them showing some isosurface of interaction. In contrast, for the Eq systems interacting from outside of the non-canonical DNA secondary structure not all the ancillary ligands are involved in the interaction. We may summarise that the Ax isomer of the  $[\text{Mo}(\eta^3\text{-C}_3\text{H}_5)\text{Br}(\text{CO})_2(\text{phen})]$  complex is more stable when interacting with the GQ through the end-stacking mode of interaction and totally inside the non-canonical DNA secondary structure than the Eq isomer interacting from outside of the non-canonical DNA secondary structure due to the larger number of weak interactions, not only with the phen ligand but also through the rest of the ligands, which produces a better stabilisation of the interaction with the non-canonical DNA secondary structure. The high number of weak interactions produced by the Br ligand in its position is specially relevant because it could be easily substituted by another halogen atom

or even another group like triflate (Tf),<sup>31</sup> which would produce the modulation of the interaction with the DNA GQ.

To finish this discussion, we would like to comment on the affinity competition and selectivity of the  $[\text{Mo}(\eta^3\text{-C}_3\text{H}_5)\text{Br}(\text{CO})_2(\text{phen})]$  complex between dDNA and GQ substrates by comparing the present results for the interaction with GQ DNA with the results obtained in our previous work for the dDNA.<sup>83</sup> In both cases, for dDNA and for the GQ, the Ax isomer has given more favourable results in energetic terms. On the other hand in both cases, interaction of the  $[\text{Mo}(\eta^3\text{-C}_3\text{H}_5)\text{Br}(\text{CO})_2(\text{phen})]$  metal complex either with the dDNA or with the GQ, the  $\Delta E_{\text{form}}$  formation energies as well as the  $\Delta E_{\text{int}}$  coming from the EDA and the  $\Delta E_{\text{aq}}$  when solvent effects are taken into account, led to results pointing towards and increase in the stability of the system when the interaction is produced with any secondary DNA structure (compare results of Fig. 3, Table 1 and Table S1 of the ESI corresponding to the current work for the GQ with their counterpart values for the dDNA found in reference 45). Thus, both DNA substrates, dDNA and GQ have excellent affinity for the interaction with the  $[\text{Mo}(\eta^3\text{-C}_3\text{H}_5)\text{Br}(\text{CO})_2(\text{phen})]$  metal complex from the energetics point of view. Nevertheless, the different absolute values for energetics regarding the interaction with the GQ are always higher than for the interaction with the dDNA, roughly twice, and therefore we believe that this  $[\text{Mo}(\eta^3\text{-C}_3\text{H}_5)\text{Br}(\text{CO})_2(\text{phen})]$  complex could be selective for the interaction with such GQ non-canonical DNA secondary structure. Moreover, both the QTAIM and the NCI analyses confirm more number of weak interactions when the  $[\text{Mo}(\eta^3\text{-C}_3\text{H}_5)\text{Br}(\text{CO})_2(\text{phen})]$  metal complex is interacting with the GQ than when it is interacting with the dDNA (compare results of Fig. 4 and 5 of the manuscript and of Tables S3 – S10 and of Figures S2 – S17 of the ESI for the GQ with the respective counterparts in ref 45 for the dDNA). In any case, in both substrates, dDNA and GQ, similar kind of weak interactions are shown in which  $\pi$ - $\pi$  stacking interactions between the phen ligand and the bases of DNA are found, whereas the ancillary ligands play also a key role in the final stabilisation of the system interacting with different parts of the DNA secondary structure depending on the mode of interaction. Thus, taking also into account all these observations of the QTAIM and NCI analyses we can affirm that the  $[\text{Mo}(\eta^3\text{-C}_3\text{H}_5)\text{Br}(\text{CO})_2(\text{phen})]$  complex may interact favourably with both DNA secondary structures, the dDNA and the GQ, but again with more affinity for the GQ and therefore with more selectivity for such non-canonical DNA secondary structure.

## Conclusions

In this work, for the first time, we have studied different interaction modes for different isomers, namely, Eq and Ax of the  $[\text{Mo}(\eta^3\text{-C}_3\text{H}_5)\text{Br}(\text{CO})_2(\text{phen})]$  metal complex when interacting with a non-canonical GQ DNA secondary structure, containing 966 atoms, by means of a LS-DFT method. We mainly analysed two interaction modes, the end-stacking mode, where the complex is completely inside the non-canonical DNA secondary structure, and the interaction from outside with DNA bases in which the intercalation of the phen ligand is the main

mode of interaction observed for the studied systems. The Ax isomer prefers the end-stacking mode of interaction, while for the Eq isomer the intercalation from outside of the non-canonical DNA secondary structure is favoured. The combined results from geometry optimisations and formation energies lead to the conclusion that the end-stacking mode of interaction of the Ax isomer between tetrads of DNA is the most stable binding mode. We assume the complexity of the process, where the GQ should be unfolded for the latter introduction of the metal complex inside the non-canonical DNA secondary structure or that the  $[\text{Mo}(\eta^3\text{-C}_3\text{H}_5)\text{Br}(\text{CO})_2(\text{phen})]$  metal complex could act as promoter and stabiliser for the formation of such GQ.

Subsequent analyses by means of EDA and solvation energies confirm that even both interaction modes are stable, if solvent effects are taken into account, end-stacking of the Ax isomer totally inside the non-canonical DNA secondary structure is the most favourable mode of interaction. Moreover, QTAIM and NCI analyses confirm that the interaction of the Ax isomer by means of end-stacking totally inside the non-canonical DNA secondary structure produces more weak interactions than the interaction of the Eq isomer intercalating from outside.

We also conclude that the  $[\text{Mo}(\eta^3\text{-C}_3\text{H}_5)\text{Br}(\text{CO})_2(\text{phen})]$  metal complex could be selective for this non-canonical GQ DNA secondary structure since the  $\Delta E_{\text{form}}$ ,  $\Delta E_{\text{int}}$  and  $\Delta E_{\text{aq}}$  energies are more negative than those for the dDNA, while weak interaction analyses show similar kind of weak interactions for both dDNA and GQ but more number of such weak interactions in the case of the GQ substrate.

## Conflicts of interest

There are no conflicts to declare.

## Acknowledgements

This research was financially supported by the Fundação para a Ciência e a Tecnologia (FCT) by means of the projects PTDC/QUI-QFI/29236/2017, UIDB/04046/2020 and UIDP/04046/2020 and by the Spanish Ministry of Economy, Industry and Competitiveness under the Maria de Maeztu Units of Excellence Programme – MDM-2016-0618. A. G. is thankful to ARAID–Fundación Agencia Aragonesa para la Investigación y el Desarrollo for current funding in the frame of ARAID researchers. The authors also thank for technical and human support provided by IZO-SGI (SGiker) of UPV/EHU and European funding (ERDF and ESF). Financial support comes also from Eusko Jaurlaritza (Basque Government) through the project IT1584-22, and grant PGC2018-099321-B-100 from the Ministry of Science, Innovation and Universities through the Office of Science Research (MINECO/FEDER). We also acknowledge PRACE for awarding us access to Marconi-KNL at CINECA, Italy. Pseudopotentials and Numerical Atomic Orbitals Basis Data set for SIESTA were provided by Simune Atomistics S. L. ([www.simuneatomistics.com](http://www.simuneatomistics.com)). I. O. d. L. is also very grateful to CIC-nanogune BRTA for his Ph.D. grant.

## References

- R. Cagan and P. Meyer, *Rethinking cancer: current challenges and opportunities in cancer research*, 2017.
- B. Rosenberg, L. Van Camp, T. Krigas, *Nature*, 1965, **205**, 698.
- C. L. Kielkopf, K. E. Erkkila, B. P. Hudson, J. K. Barton, D. C. Rees, *Nat. Struct. Biol.*, 2000, **7**, 117.
- A. Y. Lebedeva, O. A. Fedorova, V. B. Tsvetkov, V. Y. Grinberg, N. V. Grinberg, T. V. Burova, A. S. Dubovik, K. K. Babievsky, V. V. Fedorov, *Dyes Pigm.*, 2018, **157**, 80.
- A. Kellett, Z. Molphy, C. Slator, V. McKee, N. P. Farrell, *Chem. Soc. Rev.*, 2019, **48**, 971.
- S. Balasubramanian, L. H. Hurley, S. Neidle, *Nat. Rev. Drug Discov.*, 2011, **10**, 261.
- S. Neidle, *Nat. Rev. Chem.* 2017, **1**, 1.
- A. Siddiqui-Jain, C. L. Grand, D. J. Bearss, L. H. Hurley, *Proc. Natl. Acad. Sci. USA PNAS*, 2002, **99**, 11593.
- A. T. Phan, *FEBS J.* 2010, **277**, 1107.
- S. Burge, G. N. Parkinson, P. Hazel, A. K. Todd, S. Neidle, *Nucleic Acid Res.*, 2006, **34**, 5402.
- D. Bhattacharyya, G. Mirihana Arachchilage, S. Basu, *Front. Chem.* 2016, **4**, 38.
- E. Largy, J.-L. Mergny, V. Gabelica, *The Alkali Metal Ions: Their Role for Life*, Springer, 2016, pp. 203-258.
- R. Rodriguez, G. D. Pantoş, D. P. Gonçalves, J. K. Sanders, S. Balasubramanian, *Angew. Chem. Int. Ed.* 2007, **46**, 5405.
- A. Arola and R. Vilar, *Curr. Top. Med. Chem.* 2008, **8**, 1405.
- A. Gil, M. Melle-Franco, V. Branchadell, M. J. Calhorda, *J. Chem. Theory Comput.* 2015, **11**, 2714.
- A. Gil, V. Branchadell, M. J. Calhorda, *RSC Adv.*, 2016, **6**, 85891.
- A. Galliot, A. Gil, M. J. Calhorda, *Phys. Chem. Chem. Phys.* 2017, **19**, 16638.
- A. Gil, A. Sanchez-Gonzalez, V. Branchadell, *J. Chem. Inf. Model.* 2019, **59**, 3989.
- Á. Sánchez-González, T. G. Castro, M. Melle-Franco, A. Gil, *Phys. Chem. Chem. Phys.*, 2021, **23**, 26680.
- C. R. Brodie, J. G. Collins, J. R. Aldrich-Wright, *Dalton Trans.*, 2004, 1145.
- P. Prasad, P. K. Sasmal, R. Majumdar, R. R. Dighe, A. R. Chakravarty, *Inorg. Chim. Acta*, 2010, **363**, 2743.
- H.-L. Seng, S.-T. Von, K.-W. Tan, M. J. Maah, S.-W. Ng, R. N. Z. R. Abd Rahman, I. Caracelli, C.-H. Ng, *Biomaterials*, 2010, **23**, 99.
- S. Shi, X. Geng, J. Zhao, T. Yao, C. Wang, D. Yang, L. Zheng, L. Ji, *Biochimie*, 2010, **92**, 370.
- J. Sun, Y. An, L. Zhang, H.-Y. Chen, Y. Han, Y.-J. Wang, Z.-W. Mao, L.-N. Ji, *J. Inorg. Biochem.*, 2011, **105**, 149.
- G. Liao, X. Chen, J. Wu, C. Qian, H. Wang, L. Ji, H. Chao, *Dalton Trans.*, 2014, **43**, 7811.
- J.-L. Yao, X. Gao, W. Sun, S. Shi, T.-M. Yao, *Dalton Trans.*, 2013, **42**, 5661.
- K.-H. Leung, V. P.-Y. Ma, H.-Z. He, D. S.-H. Chan, H. Yang, C.-H. Leung, D.-L. Ma, *RSC Adv.*, 2012, **2**, 8273.
- L. He, X. Chen, Z. Meng, J. Wang, K. Tian, T. Li, F. Shao, *Chem. Commun.*, 2016, **52**, 8095.
- C. L. Ruehl, A. H. Lim, T. Kench, D. J. Mann, R. Vilar, *Chem. Eur. J.*, 2019, **25**, 9691.
- M. Matos, C. Romão, C. C. Pereira, S. Rodrigues, M. Mora, P. Silva, M. J. Alves, C. Reis, WO2005/087783.
- D. Bandarra, M. Lopes, T. Lopes, J. Almeida, M. S. Saraiva, M. Vasconcelos-Dias, C. D. Nunes, V. Félix, P. Brandão, P. D. Vaz, M. Meireles, M. J. Calhorda, *J. Inorg. Biochem.*, 2010, **104**, 1171.
- I. Ortiz de Luzuriaga, X. Lopez, A. Gil, *Ann. Rev. Biophys.*, 2021, **50**, 209.
- P. Wu, D.-L. Ma, C.-H. Leung, S.-C. Yan, N. Zhu, R. Abagyan, C.-M. Che, *Chem. Eur. J.*, 2009, **15**, 13008.
- R. Bonsignore, F. Russo, A. Terenzi, A. Spinello, A. Lauria, G. Gennaro, A. M. Almerico, B. K. Keppler, G. Barone, *J. Inorg. Biochem.*, 2018, **178**, 106.
- B. Rajasekhar, C. Kumar, G. Premkumar, M. A. B. Riyaz, P. Lakshmi, T. Swu, *Struct. Chem.* 2019, **30**, 727.
- G. Farine, C. Migliore, A. Terenzi, F. Lo Celso, A. Santoro, G. Bruno, R. Bonsignore, G. Barone, *Eur. J. Inorg. Chem.* 2021, **2021**, 1332.
- R. Kiełtyka, J. Fakhoury, N. Moitessier, H. F. Sleiman, *Chem. Eur. J.* 2008, **14**, 1145.
- G. M. Giambaşu, D. A. Case, D. M. York, *J. Am. Chem. Soc.* 2019, **141**(6), 2435.
- J. Ho, M. B. Newcomer, C. M.; Ragain, J. A. Gascon, E. R. Batista, J. P. Loria, V. S. Batista, *J. Chem. Theory Comput.*, 2014, **10**, 5125.
- M. Aggrawal, H. Joo, W. Liu, J. Tsai, L. Xue, *Biochem. Biophys. Res. Commun.* 2012, **421**, 671.
- W. Lee and S. Matsika, *Phys. Chem. Chem. Phys.*, 2017, **19**, 3325.
- K. G. Moghaddam, G. Giudetti, W. Sipma, S. Faraji, *Phys. Chem. Chem. Phys.*, 2020, **22**, 26944.
- A. Terenzi, R. Bonsignore, A. Spinello, C. Gentile, A. Martorana, C. Ducani, B. Högberg, A. M. Almerico, A. Lauria, G. Barone, *RSC Adv.*, 2014, **4**, 33245.
- F. Guarra, T. Marzo, M. Ferraroni, F. Papi, C. Bazzicalupi, P. Gratteri, G. Pescitelli, L. Messori, T. Biver, C. Gabbiani, *Dalton Trans.*, 2018, **47**, 16132.
- S. Elleuchi, I. Ortiz de Luzuriaga, A. Sanchez-Gonzalez, X. Lopez, K. Jarraya, M. J. Calhorda, A. Gil, *Inorg. Chem.*, 2020, **59**, 12711.
- D. M. York, T.-S. Lee, W. Yang, *J. Am. Chem. Soc.*, 1996, **118**, 10940.
- T.-S. Lee, D. M. York, W. Yang, *J. Chem. Phys.*, 1996, **105**, 2744.
- E. Artacho, D. Sánchez-Portal, P. Ordejón, A. García, J. M. Soler, *Phys. Status Solidi (b)*, 1999, **215**, 809.
- J. M. Soler, E. Artacho, J. D. Gale, A. García, J. Junquera, P. Ordejón, D. Sánchez-Portal, *J. Phys. Condens. Matter.*, 2002, **14**, 2745.
- R. F. W. Bader, *Atoms in Molecules. A Quantum Theory*, Clarendon, Oxford, UK, 1990.
- E. R. Johnson, S. Keinan, P. Mori-Sánchez, J. Contreras-García, A. J. Cohen, W. Yang, *J. Am. Chem. Soc.*, 2010, **132**, 6498.
- J. Contreras-García, E. R. Johnson, S. Keinan, R. Chaudret, J.-P. Piquemal, D. N. Beratan, W. Yang, *J. Chem. Theory Comput.*, 2011, **7**, 625.
- M. v. Hopffgarten and G. Frenking, *Wiley Interdisip. Rev.: Comput. Mol. Sci.*, 2012, **2**, 43.
- A. Sánchez-González, N. A. G. Bandeira, I. Ortiz de Luzuriaga, F. F. Martins, S. Elleuchi, K. Jarraya, J. Lanuza, X. Lopez, M. J. Calhorda, A. Gil, *Molecules* 2021, **26**, 4737.
- C. Hounsou, L. Guittat, D. Monchaud, M. Jourdan, N. Saettel, J.-L. Mergny, M.-P. Teulade-Fichou, *ChemMedChem.*, 2007, **2**, 655.
- D. Mustard and D. W. Ritchie, *Proteins: Struct. Funct. Bioinf.*, 2005, **60**, 269.
- G.-Y. Chuang, D. Kozakov, R. Brenke, S. R. Comeau, S. Vajda, *Biophys. J.*, 2008, **95**, 4217.
- K. Lee, É. D. Murray, L. Kong, B. I. Lundqvist, D. C. Langreth, *Phys. Rev. B*, 2010, **82**, 081101.
- I. Ortiz de Luzuriaga, S. Elleuchi, K. Jarraya, E. Artacho, X. López, A. Gil, *Phys. Chem. Chem. Phys.*, 2022, **24**, 11510.
- D. D. Johnson, *Phys. Rev. B*, 1988, **38**, 12807.
- P. Pulay, *Chem. Phys. Lett.*, 1980, **73**, 393.
- P. Pulay, *J. Comput. Chem.*, 1982, **3**, 556.
- J. Junquera, Ó. Paz, D. Sánchez-Portal, E. Artacho, *Phys. Rev. B*, 2001, **64**, 235111.
- L. Kleinman and D. Bylander, *Phys. Rev. Lett.*, 1982, **48**, 1425.
- N. Troullier and J. L. Martins, *Phys. Rev. B*, 1991, **43**, 8861.

- 66 C. F. Guerra, J. Snijders, G. te Velde, E. J. Baerends, *Theor. Chem. Acc.*, 1998, **99**, 391.
- 67 G. te Velde, F. M. Bickelhaupt, E. J. Baerends, C. Fonseca Guerra, S. J. van Gisbergen, J. G. Snijders, T. Ziegler, *J. Comput. Chem.*, 2001, **22**, 931.
- 68 ADF, SCM, Theoretical Chemistry, Vrije Universiteit, Amsterdam, The Netherlands, 2013, <http://www.scm.com>.
- 69 K. Kitaura and K. Morokuma, *Int. J. Quantum Chem.*, 1976, **10**, 325.
- 70 F. M. Bickelhaupt and E. J. Baerends, Reviews in computational chemistry, ed. K. B. Lipkowitz and D. B. Boyd, Wiley, 2000, vol. 15, Khon – Sham Density Functional Theory: Predicting and Understanding Chemistry, pp. 1-86
- 71 C. Lee, W. Yang, R. G. Parr, *Phys. Rev. B*, 1988, **37**, 785.
- 72 A. D. Becke, *J. Chem. Phys.*, 1993, **98**, 5648.
- 73 S. Grimme, J. Antony, S. Ehrlich, H. Krieg, *J. Chem. Phys.*, 2010, **132**, 154104.
- 74 E. van Lenthe, E.-J. Baerends, J. G. Snijders, *J. Chem. Phys.*, 1993, **99**, 4597.
- 75 E. van Lenthe, E.-J. Baerends, J. G. Snijders, *J. Chem. Phys.*, 1994, **101**, 9783.
- 76 E. van Lenthe, R. van Leeuwen, E. J. Baerends, J. G. Snijders, *Int. J. Quantum. Chem.*, 1996, **57**, 281.
- 77 S. S. van Boom, D. Yang, J. Reedijk, G. A. van der Marel, A. H.-J. Wang, *J. Biomol. Struct. Dyn.*, 1996, **13**, 989.
- 78 E. van Lenthe, J. G. Snijders, E. J. Baerends, *J. Chem. Phys.*, 1996, **105**, 6505.
- 79 E. van Lenthe, A. Ehlers, E.-J. Baerends, *J. Chem. Phys.*, 1999, **110**, 8943.
- 80 A. Klamt and G. Schüürmann, *J. Chem. Soc. Perkin Trans 2*, 1993, 799.
- 81 J. Tomasi, *Theor. Chem. Acc.*, 2004, **112**, 184.
- 82 M. J. Frisch, G. W. Trucks, H. B. Schlegel, G. E. Scuseria, M. A. Robb, J. R. Cheeseman, G. Scalmani, V. barone, G. A. Petersson, H. Nakatsuji, X. Li, M. Caricato, A. V. Marenich, J. Bloino, B. G. Janesko, R. Gomperts, B. Mennucci, H. P. Hratchian, J. V. Ortiz, A. F. Izmaylov, J. L. Sonnenberg, D. Williams-Young, F. Ding, F. Lipparini, F. Egidi, J. Goings, B. Peng, A. Petrone, T. Henderson, D. Ranasinghe, V. G. Zakrzewski, J. Gao, N. Rega, G. Zheng, W. Liang, M. Hada, M. Ehara, K. Toyota, R. Fukuda, J. Hasegawa, M. Ishida, T. Nakajima, Y. Honda, O. Kitao, H. Nakai, T. Vreven, K. Throssell, J. A. Montgomery, Jr., J. E. Peralta, F. Ogliaro, M. J. Bearpark, J. J. Heyd, E. N. Brothers, K. N. Kudin, V. N. Staroverov, T. A. Keith, R. Kobayashi, J. Normand, K. Raghavachari, A. P. Rendell, J. C. Burant, S. S. Iyengar, J. Tomasi, M. Cossi, J. M. Millam, M. Klene, C. Adamo, R. Cammi, J. W. Ochterski, R. L. Martin, K. Morokuma, O. Farkas, J. B. Foresman and D. J. Fox, *Gaussian16 Revision C.01*, 2016, Gaussian Inc. Wallingford CT.
- 83 P. J. Hay and W. R. Wadt, *J. Chem. Phys.*, 1985, **82**, 299.
- 84 A. Ehlers, M. Böhme, S. Dapprich, A. Gobbi, A. Höllwarth, V. Jonas, K. Köhler, R. Stegmann, A. Veldkamp, G. Frenking, *Chem. Phys. Lett.*, 1993, **208**, 111.
- 85 T. A. Keith, *AIMALL, version 17.11.14*, TK Gistmill Software, Overland Park, KS, 2017, [aim.tkgristmill.com](http://aim.tkgristmill.com).
- 86 S. Tsuzuki and A. Fujii, *Phys. Chem. Chem. Phys.*, 2008, **10**, 2584.
- 87 A. J. Stone, *Chem. Phys. Lett.*, 1993, **211**, 101.
- 88 Á. Sánchez-González and A. Gil, *RSC Adv.*, 2021, **11**, 1553.